

Characterization of polyanion–protein complexes by frontal analysis continuous capillary electrophoresis and small angle neutron scattering: Effect of polyanion flexibility

Toshiaki Hattori^a, Sukhbaatar Bat-Aldar^a, Ryo Kato^a, H.B. Bohidar^b, Paul L. Dubin^{c,*}

^a Department of Materials Science, Toyohashi University of Technology, Toyohashi 441-8580, Japan

^b School of Physical Sciences, Jawaharlal Nehru University, New Delhi 110067, India

^c Department of Chemistry, Indiana University–Purdue University at Indianapolis, Indianapolis, IN 46202, USA

Received 21 January 2005

Available online 19 April 2005

Abstract

The binding constant (K_{obs}) for the β -lactoglobulin–poly(vinylsulfate) (BLG–PVS) complex was measured by frontal analysis continuous capillary electrophoresis at pH values above the isoelectric point of BLG, and the persistence length (L_p) of PVS was measured by small angle neutron scattering, to examine the effect of polyelectrolyte chain stiffness on its binding efficiency to proteins. The values of K_{obs} and L_p were compared with those of BLG–PSS and BLG–PAMPS (poly(2-acrylamido-2-methylpropane-sulfonate)) reported previously. The relationship between K_{obs} and L_p was reciprocal, indicating that protein binding is enhanced by the flexibility of the polyanion, at least in the case where the net protein charge is negative. In addition, at a fixed pH, the polymer systems displayed a similar ionic strength dependence of K_{obs} . This similarity was consistent with the proposal that the binding properties of PVS and PAMPS polyanions are governed purely by electrostatic interactions and are independent of their molecular structure.

© 2005 Elsevier Inc. All rights reserved.

Keywords: Protein–polyelectrolyte; FACCE; Frontal analysis; Capillary electrophoresis; Persistence length; Complex formation

The elucidation of the interaction between proteins and polyelectrolytes is an interesting subject not only because of the biological significance of protein–DNA and protein–glycosaminoglycan interactions but also because of the applications of noncognate protein–polyelectrolyte systems [1,2]. Protein–polyelectrolyte complexes may be considered as one class of macroionic complexes that include, inter alia, oppositely charged polyelectrolyte complexes (both soluble polyion complexes and polyelectrolyte multilayers), micelle–polyelectrolyte complexes, and other polyelectrolyte–colloid systems such as polyelectrolyte–dendrimer complexes and complexes of polyelectrolytes with metal oxides or hydroxides. On the other

hand, polyelectrolyte–protein complexes are unique in that they arise from the reaction between a three-dimensionally fixed and heterogeneously charged macroion (protein) and a flexible chain (Gaussian coil) strand of ionic repeat units. They demonstrate the somewhat unusual effect of strong binding even when both macroionic species have the same net charge. This consistent behavior is considered to arise from “patch binding” in which the flexible polyion “selects” the positively charged domain of the protein as the binding site [3,4]. Because proteins typically have inhomogeneous distributions of positive and negative surface charges, the repulsion between like charges is overcome by the attraction between the positive part of the protein and the negative charges of the polyelectrolyte [5,6]. On the other hand, such patch binding may, in principle, coexist with short-range interactions,

* Corresponding author. Fax: +1 317 274 6879.

E-mail address: dubin@chem.iupui.edu (P.L. Dubin).

that is, hydrophobic interactions [1,5] or hydrogen bonding [7]. However, it is unclear whether short-range interactions are ubiquitous in protein–polyelectrolyte complexes. This issue also can be related to the distinction between “strong,” “specific,” “high-affinity,” or “selective” binding, on the one hand, and “loose,” “nonspecific,” “low-affinity,” or “nonselective” binding, on the other.

The role of the electrostatic effect on protein–polyelectrolyte interaction can be assessed from the ionic strength dependence of complex formation; electrostatic forces are screened by small ions, whereas hydrophobic interactions and hydrogen bonds are enhanced and unaffected, respectively. The use of synthetic polyanions, as compared with biopolyelectrolytes, facilitates the systematic examination of the effects of charge density and chain. Previously, we measured [8] binding between β -lactoglobulin (BLG)¹ and poly(styrenesulfonate) (PSS), and poly(2-acrylamido-2-methylpropanesulfonate) (PAMPS) as a function of ionic strength, using turbidimetry and frontal analysis continuous capillary electrophoresis (FACCE) [9,10]. FACCE is conceptually very close to capillary electrophoresis/frontal analysis (CE/FA) [11] but is technically simpler. Like isotachopheresis (ITP), zone electrophoresis (CZE), isoelectric focusing (IEF), and moving boundary electrophoresis (MBE), FACCE is a form of substrate-free electrophoresis but most nearly resembles MBE in that only the fast-moving component is measured and characterized; in contradistinction, in the ITP mode, all ions at steady state travel with the same velocity [12]. We deduced binding constants (K_{obs}) from the FACCE binding isotherms via the McGhee–von Hippel model [13]. Interestingly, the K_{obs} values for the BLG–PSS complex at pH 7 showed plateaus or maxima as a function of ionic strength I in the range $10 \text{ mM} < I < 100 \text{ mM}$. This non-monotonic behavior was quite different from predictions from the model of protein–DNA binding developed by Record et al. [14]. On the other hand, an electrostatic treatment by Rubinstein and co-workers [15] provides a zeroth-order explanation of this nonlinear behavior. This model, which treats the protein as an electrical dipole, gives the interaction energy due to screened coulombic attraction and repulsion as

$$U = -\frac{Q_p}{2\epsilon} \left(\frac{Q_+}{R_+} \exp(-\kappa R_+) - \frac{Q_-}{R_-} \exp(-\kappa R_-) \right), \quad (1)$$

where Q_p , Q_+ , and Q_- are effective charges of the polyanion binding unit, the positive protein binding domain, and the negative protein domain, respectively; R_+ and R_- are distances between Q_p and Q_+ and between Q_p and Q_- , respectively (of necessity, $R_+ < R_-$); and $1/\kappa$ is the Debye length. The value of Q_- is obtained by removing all positive charges of the protein and summing the remaining negative ones (and likewise for Q_+), and the distance between Q_+ and Q_- is obtained from the centers of mass of the positive and negative charges, respectively [8]. Although the nonmonotonic behavior of K_{obs} versus I was explained by Eq. (1), no explanation was offered for the increase in K_{obs} for PSS versus PAMPS that could arise either from the smaller chain flexibility of PAMPS or from hydrophobic interaction between BLG and PSS. On the one hand, the aromatic rings of PSS have often been implicated as hydrophobic moieties [16–21]; on the other hand, PSS has frequently been considered a model polyelectrolyte [20–24], that is, without the anomalous behavior that one might expect from an amphiphilic polymer. The situation is even further complicated by the presence of unsulfonated units in some PSS samples [25]. For this reason, it appeared to be desirable to decouple the effect of chain flexibility from hydrophobic effects.

In this article, we measured by FACCE the binding constant between BLG and poly(vinylsulfate) (PVS), a vinyl polymer with the same charge density as PSS and PAMPS but with a high degree of chain flexibility. We assessed this chain flexibility by determining the persistence length with small angle neutron scattering (SANS) and demonstrating that it is indeed more flexible than PAMPS. Because neither PVS nor PAMPS has hydrophobic groups, contributions of chain stiffness to the binding constant can be resolved without possible complications from hydrophobic interactions with the protein.

Materials and methods

Reagents and solutions

BLG-A and BLG-B (cat. no. L-2506) were purchased from Sigma Chemical (St. Louis, MO, USA). PVS (polymerization degree 1500, esterification degree 98.1%) was purchased from Wako Chemicals (Richmond, VA, USA). The potassium PVS was ion-exchanged into sodium PVS using a long column packed with sodium-type cation exchange resin. The sodium-type resin was prepared from hydrogen-type AG-50W (cat. no. 42-1431, Bio-Rad, Hercules, CA, USA).

Sample solutions were made from freshly prepared stock solutions of BLG and polyelectrolyte that were dissolved in capillary electrophoresis run buffer solution.

¹ Abbreviations used: BLG, β -lactoglobulin; PSS, poly(styrenesulfonate); PAMPS, poly(2-acrylamido-2-methylpropanesulfonate); FACCE, frontal analysis continuous capillary electrophoresis; CE/FA, capillary electrophoresis/frontal analysis; ITP, isotachopheresis; CZE, zone electrophoresis; IEF, isoelectric focusing; MBE, moving boundary electrophoresis; PVS, poly(vinylsulfate); SANS, small angle neutron scattering; SEC, size exclusion chromatography.

The run buffer solution contained 10 mM phosphate salt as the pH buffer, and I was further adjusted with the addition of sodium chloride. In the complex mixture solutions, the concentration range of BLG was 0.8–4.0 g/L and the concentration of polyelectrolyte was constant at 0.2 g/L. This 4 to 20× weight excess of protein is considered sufficient to ensure the absence of free polyelectrolyte in sample, so that the faster migrating ligand (protein) reflects the concentration of free protein in the sample, an essential approximation for the validity of FACCE.

Apparatus and procedure for FACCE

Capillary electrophoresis was performed using a high-voltage supplier (HCZE-30P, no. 25, Matsusada Precision, Japan), a UV detector (CV⁴ capillary electrophoresis absorbance detector, Isco, USA), and an X-Y recorder (WX4309, Graphtec, Japan). All operating conditions were as follows: 6–8 kV of applied voltage, 214 nm of UV detector, at room temperature. The fused silica capillary (cat. no. 1010-31942, GL Sciences, Japan) with dimensions of 75 μm \times 50 cm (effective length 20 cm) was prepared prior to each set of experiments by washing with 0.1 N sodium hydroxide for 1 h, followed by a 30 min wash with water.

The FACCE experiment was initialized by equilibrating the capillary with buffer solution for 5 min. The inlet end of the capillary was then placed in a vial containing the equilibrated sample solution, and the outlet end was placed in a vial containing buffer solution. Constant voltage was applied, and separation (manifested in continuous plateaus) was observed. Typically, the first eluting plateau was the unbound protein, and the second was the protein–polyelectrolyte complex. However, at high ionic strength, the second plateau also indicated the unbound protein (Fig. 1). After each electrophoretic run, a 5 min wash with 0.1 N sodium hydroxide, followed by a 5 min rinse with water, was performed. The concentration of unbound protein was determined from the height of the plateau using a calibration curve

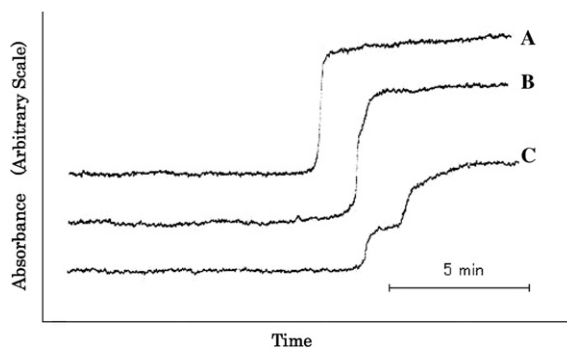


Fig. 1. Electropherograms of 0.04 g/L β -lactoglobulin at pH 6.1: (A) $I = 0.02$ M; (B) $I = 0.05$ M; (C) $I = 0.1$ M.

constructed by measuring the plateau height of known concentrations of protein obtained under the same experimental conditions as for the protein–polyelectrolyte mixture. The extent of binding—that is, the number of protein molecules bound per polymer residue (ν)—was determined from the amount of unbound and the total amount used.

Apparatus and procedure for SANS

SANS experiments were performed on the spectrometer at the GT laboratory, Dhruva reactor (Bhaba Atomic Research Centre, Trombay, India). Further details of the SANS spectrometer at Dhruva are discussed in [26]. The wavelength of the neutrons used covered the scattering vector (q) range

$$7 \times 10^{-4} \leq q \leq 3 \times 10^{-2} \text{ (nm)}^{-1}$$

given by $q = (4\pi/\lambda)\sin\theta/2$, where θ is the scattering angle, and λ is the neutron wavelength. The polymer solution prepared in D₂O was transformed to quartz cell of 2 mm thickness, and scattered intensity was measured as function scattering vector. The measured intensity was corrected for the background and the empty cell contribution, and then the data were normalized to obtain the structure factors, $S(q)$. Details of the data normalization procedure are discussed in [27].

Results and discussion

Electropherograms of BLG

FACCE electropherograms of BLG at several ionic strengths at pH 6.1 are shown in Fig. 1. The electropherograms display a single plateau at $I = 0.02$ M and two plateaus at $I = 0.1$ M. To explain the latter result, we first considered the possibility of a BLG monomer–dimer equilibrium. The literature on this matter is ambiguous; SANS has indicated that BLG at neutral pH consists of monomers and dimers [28], but size exclusion chromatography (SEC) measurements reduced to universal curves for partition coefficients have yielded a molecular weight corresponding to dimer [29], whereas SEC coupled with multiangle laser light scattering has indicated not only dimers but also monomers and higher oligomers [30]. These apparently conflicting reports may reflect coupling of a monomer–dimer equilibrium with dimer aggregation, itself a complex function of pH, I , and protein concentration [31], but light scattering indicates essentially only dimer at pH 6.1, $I = 0.2$ [32]. Finally, CZE of BLG has shown a single peak with no separation of monomers and dimers [33], unsurprising given that the charge/mass ratios of dimer and monomer should be nearly the same. On the other hand, a mixture of BLG-A and BLG-B (i.e., AA and BB dimers) should

be separable by capillary electrophoresis because in BLG-A aspartic acid replaces glycine in one of the two variant points of BLG-B [31], rendering its effective charge more negative (reported pI values of 5.13 and 5.23 for BLG-A and BLG-B, respectively) [34]. Because the electroosmotic flow is anodic, BLG-B elutes earlier than BLG-A [12,32], and in FACCE electropherograms the plateau for BLG-B should be followed by mixed BLG. Ionic strength facilitates the separation by decreasing mobility, either by decreasing effective charge or by enhancing adsorption onto the capillary column.

The separation noted above allows calibration curves of BLG-B and total BLG; both of these were linear, so that both the unbound BLG-B and the unbound BLG_{total} concentrations could be measured in solution with PVS. Using the comparison between the relative ratios of free BLG-B to free BLG_{total} in the complex and in polymer-free BLG, it was possible to determine the binding properties of BLG-B. The average ratio in the complexes was 0.38 ± 0.01 compared with 0.40 ± 0.02 in a polymer-free solution. Because these ratios are nearly equal within experimental error, the binding constants for BLG-B and BLG_{total} also must be approximately the same. In the current studies, all binding data pertain to BLG_{total} and the results are compared with similar previously reported data [8].

BLG–PVS binding isotherms and binding parameters

Binding isotherms of BLG–PVS at pH 6.1 are shown in Fig. 2, where L_{free} is the molar concentration of unbound BLG and v is the number of protein molecules

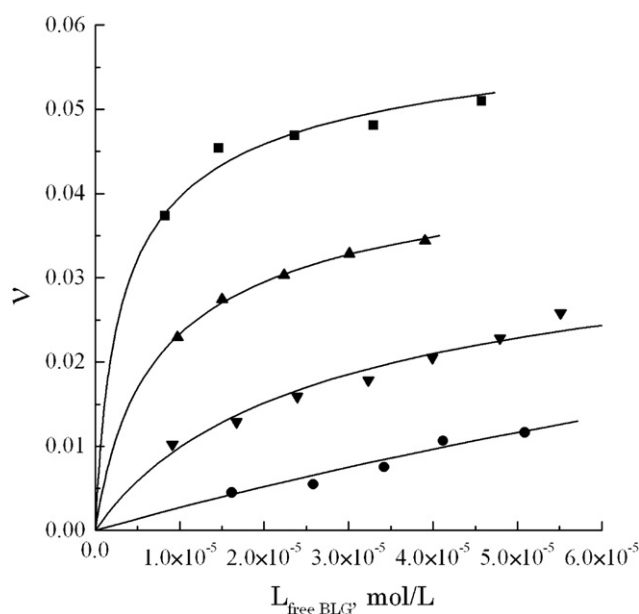


Fig. 2. Binding isotherms of BLG–PVS at pH 6.1: ■, $I = 0.01$; ▲, $I = 0.02$; ▼, $I = 0.05$; ●, $I = 0.1$.

bound per polymer residue. The amount of bound BLG (v) decreases with ionic strength, as expected for an electrostatic association. In the measured regions, all binding isotherms were simple convex, with the radius of curvature increasing with ionic strength. This indicated that BLG–PVS, like BLG–PAMPS, exhibits noncooperative binding.

The data in Fig. 2 were least-squares fitted (solid lines) to the McGhee–von Hippel equation [10]:

$$\frac{v}{L_{free}} = K_{obs}(1 - nv) \left(\frac{1 - nv}{1 - (n-1)v} \right)^{n-1}, \quad (2)$$

where K_{obs} is the binding constant and n is the number of polymer repeat units per bound protein. In the protein–polyelectrolyte system, the binding site size does not define the nature of the bound polyelectrolyte segments; rather, it indicates the typical length of polyelectrolyte occupied by one protein [35]. The fitting parameters for the BLG–PVS system are listed in Table 1. Although the binding constants were obtained precisely, the binding site size parameters had to be estimated with less accuracy. Nevertheless, it was found that K_{obs} did not significantly depend on n . Except for the data at $I = 0.1$, n ranges from 13 to 18 (i.e., on the order of 4–5 nm). This indicates that PVS cannot wind tightly around a 6-nm BLG dimer. As mentioned previously, dimers might coexist with monomers, and binding to polymer might perturb the monomer–dimer equilibrium, so that BLG monomers might be bound. If the molecular weight of the monomer is used, the binding constant remains the same but the value of the site size is halved. Even in this case, a subunit of PVS with a contour length of 2.5 nm can topologically wind around a BLG monomer of equal dimensions. Electrostatic computer modeling of the surface charge distribution of monomer BLG [5] shows a distinct positively charged region. Our observation suggests a complex in which the chain of PVS segments is not strongly deformed relative to that of isolated polymer and interacts only with a discrete positive protein domain.

Table 1
Binding parameter of BLG–PVS

	I	$\log K_{obs}$	n
pH 6.1	0.01	4.33 ± 0.09	13.1 ± 0.7
	0.02	3.82 ± 0.02	16.3 ± 0.3
	0.05	3.17 ± 0.05	17.9 ± 2.2
	0.10	2.45 ± 0.07	8.4 ± 8.3
pH 6.3	0.01	3.23 ± 0.03	16.1 ± 1.4
	0.03	3.05 ± 0.05	14.5 ± 3.1
	0.05	2.78 ± 0.04	13.0 ± 4.6
	0.07	2.67 ± 0.01	14.3 ± 1.1

Flexibility of PVS and ionic strength dependence of binding constants

Polyelectrolyte flexibility is expressed through the persistence length (L_p), which in turn controls its binding with complementary macroions. PAMPS is a well-characterized polyelectrolyte and resembles PVS except that PAMPS has a higher persistence length. Also, both PVS and PAMPS are nonhydrophobic molecules. Because data for L_p of PAMPS have already been reported [36], whereas data for L_p of PVS have not, we measured the latter using SANS. Fig. 3 shows the measured $S(q)$ data at 0.5 M NaCl solution, which is analyzed within the framework of the Kratky–Porod model [37]. According to this model, the polymer chain is composed of segments of length l_k , where l_k is the Kuhn segment length [38] and $l_k \approx 2l_p$. Here, l_p is the persistence length of the polymer that can be deduced from SANS experiments. This model stipulates that the structure factor scales as $S(q) \sim q^{-2}$ for a Gaussian coil, whereas for rod-like structures $S(q) \sim q^{-1}$. The transition from flexible to rod-like behavior will be seen at a characteristic wave vector q^* , called the Kratky–Porod cutoff, given by $q^* \approx 6/(\pi l_p)$. (3)

The plots of slopes -2 and -1 intersect at q^* , and from the diagram shown in Fig. 3, $q^* \approx 0.0633^{-1}$ (nm), giving persistence length $l_p \approx (3.0 \pm 0.2)$ nm, corresponding to Kuhn segment length $l_k \approx 6$ nm. It is also possible to find out characteristic ratio $C_\infty = (2l_p/I_{\text{chem}}) - 1 = 3.8 \pm 0.2$, where the monomer unit bond length for vinyl polymers $I_{\text{chem}} = 0.154$ nm is used. At the same ionic strength, the persistence length value for PVS was 3.0 nm and was smaller than that for PAMPS (5.1 nm). Therefore, the order of the persistence length is PVS < PAMPS. Regarding the binding to BLG, however, studies of other complexes between polyelectrolytes and proteins, micelles, or dendrimers [39,40] indicate that one should use either a bare

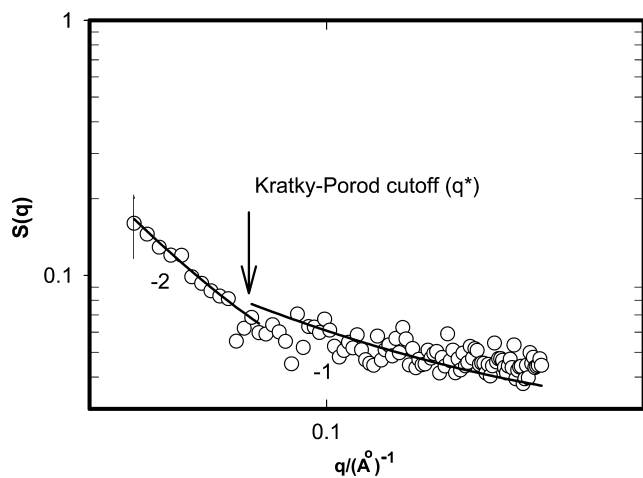


Fig. 3. Relation between $S(q)$ and $q/(\text{Å}^{-1})^{-1}$ for PVS in 0.5 M NaCl. A representative error bar is shown for one of the data points.

persistence length L_0 or some intermediate value between that and the total persistence length L_p . In the Odijk–Skolnick–Fixman formulation [41,42], L_p is the sum of L_0 and an electrostatic contribution, L_e :

$$L_p = L_0 + L_e. \quad (4)$$

L_e depends on intramolecular electrostatic forces and is empirically approximated by $L_e \sim I^{1/2}$, so that L_0 can be determined by linear extrapolation to infinite ionic strength. For PAMPS, $L_0 \approx 2.4$ nm $\approx L_p/2$ [36]. The ionic strength dependence should be similar, allowing us to retain the flexibility order PVS > PAMPS.

The ionic strength dependences of K_{obs} for PVS, PAMPS, and PSS are shown in Fig. 4. The very large increase in K_{obs} for both PVS and PAMPS when the pH decreases minutely from 6.3 to 6.1 must be explained by the powerful influence of the ionization state of a few amino acids, most likely basic amino acids located in the positive patch of BLG [5]. At both pH values, K_{obs} is substantially larger for PVS than for PAMPS (in the order of flexibility), with hydrophobic interactions not likely to be relevant for either polymer. It is also worth noting that the curves at pH 6.2 for PAMPS and PVS are essentially parallel, with $dK_{\text{obs}}/d \log I$ being independent of the structural features of the two polyanions, suggesting the primacy of long-range electrostatic forces. Regarding the data for PSS, it is difficult to exclude the possibility of a hydrophobic force. The hydrophobic interaction increases with ionic strength, consistent with the shape of that curve in Fig. 4, but

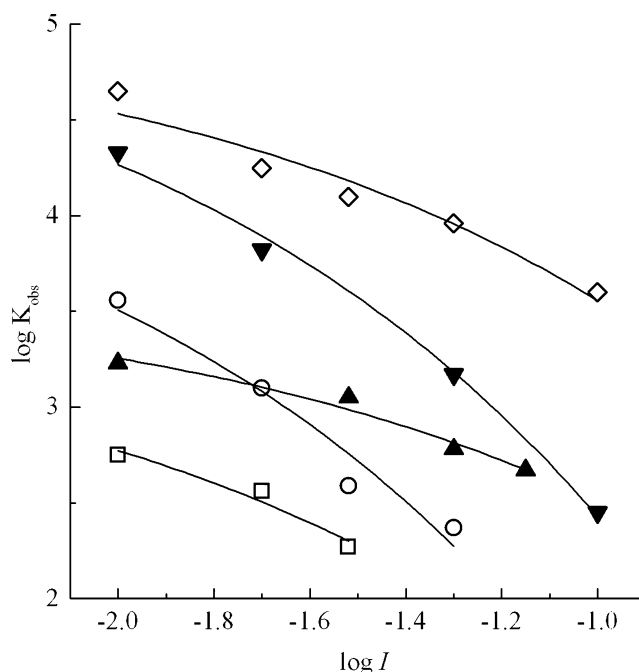


Fig. 4. Effect of ionic strength on BLG–polyanion binding constants: \blacktriangle , PVS at pH 6.3; \square , PAMPS at pH 6.3; \diamond , PSS at pH 6.3; \blacktriangledown , PVS at pH 6.1; \circ , PAMPS at pH 6.1. The data for PSS and PAMPS are from [8].

these effects are usually observed only at higher salt concentrations [43].

The electrostatic interaction model proposed by Eq. (1) is simple, and this allows explicit features of the binding mechanism to be explained [8]. With regard to Eq. (1), the ability of chain flexibility to maximize attraction and minimize repulsion would lead to a decrease in R_+ and/or an increase in R_- . Fig. 5 shows the electrostatic energy as a function of these distances. The inputs used were $R_- = 1.5$ nm and $Q_-/Q_+ = 1.1$, with $R_+ = 1.0$, 1.05, and 1.1 nm for A, B, and C, respectively. The binding energy is clearly very sensitive to R_+ . Similar sensitivity was seen with variations of R_- . Although the ranges chosen for R_+ , R_- , and Q_-/Q_+ represent a simplification of a much more complex problem, the dependence of electrostatic-free energy on ionic strength is clear. Figs. 4 and 5 also reveal qualitative similarity that supports the patch binding mechanism. Even if Q_-/Q_+ is not physical, it should be nearly independent of ionic strength. Therefore, the close resemblance between the ionic strength dependence of the binding constants in Fig. 4 and the model curves shown in Fig. 5 suggests that for PVS and PAMPS, nonelectrostatic interactions play a minor role during the binding process. Of course, the release of small ions that accompanies intermacro-ionic complexation may contribute a favorable entropy component to the binding energy, but because this effect is inextricably linked to the coulombic stabilization of a bound state embodied in Eq. (1), we do not consider this to be a nonelectrostatic interaction.

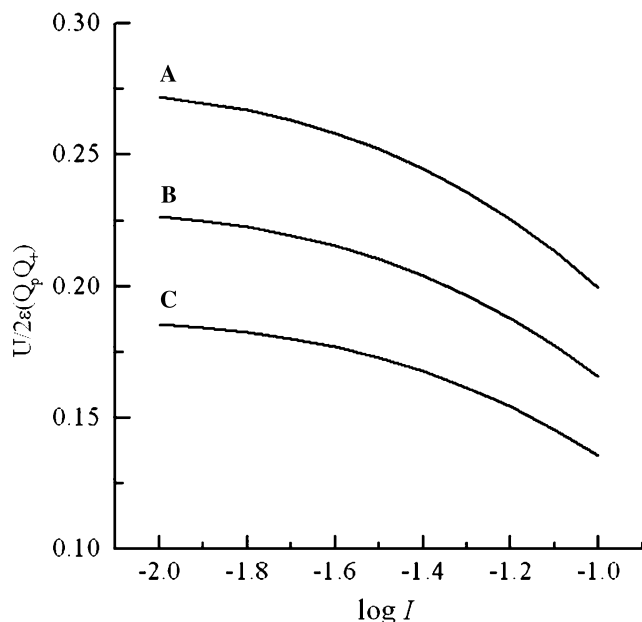


Fig. 5. Electrostatic potential energies of the BLG-polyanion calculated from the patch binding Eq. (1). The input conditions are (A) $R_+ = 1$ nm, $R_- = 1.5$ nm, $Q_-/Q_+ = 1.1$; (B) $R_+ = 1.05$ nm, $R_- = 1.5$ nm, $Q_-/Q_+ = 1.1$; and (C) $R_+ = 1.1$ nm, $R_- = 1.5$ nm, $Q_-/Q_+ = 1.1$.

Conclusions

FACCE results indicated that the binding of BLG for two polyanions, PVS and PAMPS, is strongly dependent on ionic strength and remarkably sensitive to pH. Nevertheless, at all conditions K_{obs} for PVS was larger than that for PAMPS, typically by a factor of 5 or 10. The persistence length L_p of PVS was determined by SANS and found to be significantly smaller than that of PAMPS. These results demonstrated an inverse relation between K_{obs} and L_p , indicating that protein binding was enhanced by polyanion flexibility. The general shapes of $\log K_{\text{obs}}$ versus $\log I$ were similar for these two polyanions, suggesting a common electrostatic origin. K_{obs} of PSS was significantly larger than K_{obs} for PVS or PAMPS, although the persistence length of PASS was close to that of PVS. Whether this effect arises from a hydrophobic interaction is not clear.

Acknowledgment

Supported from the National Science Foundation (CHE-0345382) is acknowledged.

References

- [1] C. Tribet, Complexation between amphiphilic polyelectrolytes and proteins: from necklaces to gels, in: T. Radeva (Ed.), *Physical Chemistry of Polyelectrolytes*, Marcel Dekker, New York, 2001, pp. 687–741.
- [2] J. Xia, P. Dubin, Protein-polyelectrolyte complexes, in: P. Dubin, J. Bock, R.M. Davies, D.N. Schulz (Eds.), *Macromolecular Complexes in Chemistry and Biology*, Springer-Verlag, Berlin, 1994, pp. 247–271.
- [3] J.M. Park, B.B. Muhoberac, P.L. Dubin, J. Xia, Effect of protein charge heterogeneity in protein-polyelectrolyte complexation, *Macromolecules* 25 (1992) 290–295.
- [4] K.M. Mattison, P.L. Dubin, I.J. Brittain, Complex formation between bovine serum albumin and strong polyelectrolytes: effect of polymer charge density, *J. Phys. Chem. B* 102 (1998) 3830–3836.
- [5] E. Seyrek, P.L. Dubin, C. Tribet, E.A. Gamble, Ionic strength dependence of protein-polyelectrolyte interactions, *Biomacromolecules* 4 (2003) 273–282.
- [6] K.R. Grymonpre, B.A. Staggemeier, P.L. Dubin, K.M. Mattison, Identification by integrated computer modeling and light scattering studies of an electrostatic serum albumin-hyaluronic acid binding site, *Biomacromolecules* 2 (2001) 422–429.
- [7] J. Xia, P.L. Dubin, E. Kokufuta, Dynamic and electrophoretic light scattering of a water-soluble complex formed between pepsin and polyethylene glycol, *Macromolecules* 26 (1993) 6688–6690.
- [8] T. Hattori, R. Hallberg, P.L. Dubin, The roles of electrostatic interaction and polymer structure in the binding of β -lactoglobulin to anionic polyelectrolytes: measurement of binding constants by FACCE, *Langmuir* 16 (2000) 9738–9743.
- [9] J.Y. Gao, P.L. Dubin, B.B. Muhoberac, Measurement of the binding of proteins to polyelectrolytes by frontal analysis continuous capillary electrophoresis, *Anal. Chem.* 69 (1997) 2945–2951.

- [10] R.M. Guijt-van Duijn, J. Frank, G.W.K. van Dedem, E. Baltussen, Recent advances in affinity capillary electrophoresis, *Electrophoresis* 21 (2000) 3905–3918.
- [11] (a) J.C. Kraak, S. Busch, H. Poppe, Study of protein–drug binding using capillary zone electrophoresis, *J. Chromatogr.* 608 (1992) 257–264;
(b) T. Ohara, A. Shibukawa, T. Nakagawa, Capillary electrophoresis/frontal analysis for microanalysis of enantioselective protein binding of a basic drug, *Anal. Chem.* 67 (1995) 3520–3525;
(c) P.A. McDonnell, G.W. Caldwell, High performance capillary electrophoresis/frontal analysis of drugs binding to human serum proteins and human serum, in: A.-U. Rahman (Ed.), *New Advances in Analytical Chemistry*, Harwood Academic, Amsterdam, Netherlands, 2000;
(d) P.A. McDonnell, G.W. Caldwell, J.A. Masucci, Using capillary electrophoresis/frontal analysis to screen drugs interacting with human serum proteins, *Electrophoresis* 19 (1998) 448–454;
(e) Y.S. Fung, D.X. Sun, C.Y. Yeung, Capillary electrophoresis for determination of free and albumin-bound bilirubin and the investigation of drug interaction with bilirubin-bound albumin, *Electrophoresis* 21 (2000) 403–410.
- [12] J.W. Jorgenson, *Electrophoresis*, *Anal. Chem.* 58 (1986) A743–A760.
- [13] J.D. McGhee, P.H. von Hippel, Theoretical aspects of DNA–protein interaction: co-operative and non-co-operative binding of large ligands to a one dimensional homogeneous lattice, *J. Mol. Biol.* 86 (1974) 469–489.
- [14] M.T. Record Jr., C.F. Anderson, T.M. Lohman, Thermodynamic analysis of ion effects on the binding and conformational equilibria of proteins and nucleic acids: the roles of ion association or release, screening, and ion effects on water activity, *Q. Rev. Biophys.* 11 (1976) 103–178.
- [15] W.A. Bowman, M. Rubinstein, J.S. Tan, Polyelectrolyte–gelatin complexation: light-scattering study, *Macromolecules* 30 (1997) 3262–3270.
- [16] N.J. Turro, T. Okubo, Microscopic environment of poly(styrenesulfonate) macroanions: emission and absorption spectra, lifetime, and depolarization measurements of a cationic fluorescence probe under high pressure, *J. Am. Chem. Soc.* 104 (1982) 2985–2988.
- [17] N.J. Turro, T. Okubo, C.-J. Chung, J. Emert, R. Catena, Polyelectrolyte-enhanced excimer formation of bis(α -naphthylmethyl) ammonium chloride and (α -naphthylmethyl) ammonium chloride, *J. Am. Chem. Soc.* 104 (1982) 4799–4803.
- [18] K. Hayakawa, J.C.T. Kwak, Surfactant–polyelectrolyte interactions: I. Binding of dodecyltrimethylammonium ions by sodium dextran sulfate and sodium poly(styrenesulfonate) in aqueous solution in the presence of sodium chloride, *J. Phys. Chem.* 86 (1982) 3866–3870.
- [19] Z. Gao, J.C.T. Kwak, R.E. Wasylshen, An NMR study of the binding between polyelectrolytes and surfactants in aqueous solution, *J. Colloid Interface Sci.* 126 (1988) 371–376.
- [20] S. Mori, Secondary effects in aqueous size exclusion chromatography of sodium poly(styrene sulfonate) compounds, *Anal. Chem.* 61 (1989) 530–534.
- [21] P. Molyneux, *Water Soluble Synthetic Polymers*, vol. 2, CRC Press, Boca Raton, FL, 1984.
- [22] R.S. Koene, M. Mandel, Scaling relations for aqueous polyelectrolyte–salt solutions: I. Quasi-elastic light scattering as a function of polyelectrolyte concentration and molar mass, *Macromolecules* 16 (1983) 220–227.
- [23] L. Wang, H. Yu, Chain conformation of linear polyelectrolyte in salt solutions: sodium poly(styrenesulfonate) in potassium chloride and sodium chloride, *Macromolecules* 21 (1988) 3498–3501.
- [24] J. Yamanaka, H. Matsuoka, H. Kitano, M. Hasegawa, N. Ise, Viscosity behavior of salt-free aqueous solutions of sodium poly(styrenesulfonates), *J. Am. Chem. Soc.* 112 (1990) 587–592.
- [25] B. Zhang, T. Hattori, P.L. Dubin, Observation of compositional heterogeneity in poly(styrenesulfonate) using frontal analysis continuous capillary electrophoresis, *Macromolecules* 34 (2001) 6790–6794.
- [26] V.K. Aswal, P.S. Goyal, Small-angle neutron scattering diffractometer at Dhruva reactor, *Curr. Sci.* 79 (2000) 947–952.
- [27] P. Thiagarajan, J.E. Epperson, R.K. Crawford, J.M. Carpenter, T.E. Klippert, D.G. Wozniak, The time-of-flight small-angle neutron diffractometer (SAD) at IPNS, Argonne National Laboratory, *J. Appl. Crystallogr.* 30 (1997) 280–293.
- [28] M. Verheul, J.S. Pederson, S.P.F.M. Roefs, K.G. de Kruijff, Association behavior of native β -lactoglobulin, *Biopolymers* 49 (1997) 11–20.
- [29] (a) R.C. Tarvers, F.C. Church, Use of high-performance size-exclusion chromatography to measure protein molecular weight and hydrodynamic radius, *Int. J. Pept. Protein Res.* 26 (1985) 539–549;
(b) P. Frigon, J.K. Leypolt, S. Uyeji, L.W. Henderson, Disparity between Stokes radii of dextrans and proteins as determined by retention volume in gel permeation chromatography, *Anal. Chem.* 55 (1983) 1349–1354.
- [30] J.A.P.P. van Dijk, J.A.M. Smit, Size-exclusion chromatography–multiangle laser light scattering analysis of β -lactoglobulin and bovine serum albumin in aqueous solution with added salt, *J. Chromatogr. A* 867 (2000) 105–112.
- [31] R. Ganta, P. Mahji, R. Vanam, E. Seyrek, P.L. Dubin, Electrostatically-driven reversible aggregation of β -lactoglobulin. *Langmuir* (submitted).
- [32] G.R. Paterson, J.P. Hill, D.E. Otter, Separation of β -lactoglobulin A, B, and C variants of bovine whey using capillary zone electrophoresis, *J. Chromatogr. A* 700 (1995) 105–110.
- [33] H.L. Monaco, G. Zanotti, P. Sadon, M. Bolognesi, L. Sawyer, E.E. Eliopoulos, Crystal structure of the trigonal form of bovine β -lactoglobulin and of its complex with retinol at 2.5 Å resolution, *J. Mol. Biol.* 197 (1987) 695–706.
- [34] S. Fredriksson, Scanning isoelectric focusing in small density gradient columns: II. Microfraction of column contents—Evaluation of pH course: isoelectric points of—lactoglobulins A and B, *Anal. Biochem.* 50 (1972) 575–585.
- [35] T. Hattori, K. Kimura, E. Seyrek, P.L. Dubin, Binding of bovine serum albumin to heparin determined by turbidimetric titration and frontal analysis continuous capillary electrophoresis, *Anal. Biochem.* 295 (2001) 158–167.
- [36] M. Tricot, Comparison of experimental and theoretical persistence length of some polyelectrolytes at various ionic strengths, *Macromolecules* 17 (1984) 1698–1704.
- [37] (a) D.I. Svergun, L.A. Feigin, X-ray and Neutron Low-Angle Scattering [Rentgenovskoe i Neitronnoe Malouglovoe Rasseyanie], Nauka, Moscow, USSR, 1986;
(b) O. Kratky, G. Porod, X-ray investigation of dissolved chain molecules, *Rec. Trav. Chim. Pays-Bas* 68 (1949) 1106–1122.
- [38] W. Kuhn, The shape of fibrous molecules in solutions, *Kolloid-Z.* 68 (1934) 2–15.
- [39] A.B. Kayitmazer, E. Seyrek, P.L. Dubin, B.A. Staggemeier, Influence of chain stiffness on the interaction of polyelectrolytes with oppositely charged micelles and proteins, *J. Phys. Chem. B* 107 (2003) 8158–8165.
- [40] A.G. Kayitmazer, D. Shaw, P.L. Dubin, The role of polyelectrolyte persistence length in the binding of oppositely charged micelles, dendrimers, and protein to chitosan and poly(dimethylallylammonium chloride), *Macromolecules* (accepted for publication).

- [41] T. Odijk, Polyelectrolyte near the rod limit, *J. Polym. Sci. Phys. Ed.* 15 (1977) 477-483.
- [42] J. Skolnick, M. Fixman, Electrostatic persistence length of a wormlike polyelectrolyte, *Macromolecules* 10 (1977) 944-948.
- [43] (a) S. Shaltiel, G. Halperin, Hydrophobic chromatography using homologs series of alkylagaroses: mechanistic considerations, *Proc. FEBS Meet.* (1979) 441-451;
(b) S. Shaltiel, Hydrophobic chromatography, *Methods Enzymol.* 104 (1984) 69-96.